

SAND REPORT

SAND2002-0772
Unlimited Release
Printed April/2002

Final Report for SEED Project (1218): "Inexpensive Chemresistor Sensors for Real Time Ground Water Contamination Measurement"

Robert C. Hughes(PI), Chad E. Davis, and Michael L. Thomas

Prepared by
Sandia National Laboratories
Albuquerque, New Mexico 87185 and Livermore, California 94550

Sandia is a multiprogram laboratory operated by Sandia Corporation,
a Lockheed Martin Company, for the United States Department of
Energy under Contract DE-AC04-94AL85000.

Approved for public release; further dissemination unlimited.



Sandia National Laboratories

Issued by Sandia National Laboratories, operated for the United States
Department of Energy by Sandia Corporation.

NOTICE: This report was prepared as an account of work sponsored by an agency of the United States Government. Neither the United States Government, nor any agency thereof, nor any of their employees, nor any of their contractors, subcontractors, or their employees, make any warranty, express or implied, or assume any legal liability or responsibility for the accuracy, completeness, or usefulness of any information, apparatus, product, or process disclosed, or represent that its use would not infringe privately owned rights. Reference herein to any specific commercial product, process, or service by trade name, trademark, manufacturer, or otherwise, does not necessarily constitute or imply its endorsement, recommendation, or favoring by the United States Government, any agency thereof, or any of their contractors or subcontractors. The views and opinions expressed herein do not necessarily state or reflect those of the United States Government, any agency thereof, or any of their contractors.

Printed in the United States of America. This report has been reproduced directly from the best available copy.

Available to DOE and DOE contractors from
U.S. Department of Energy
Office of Scientific and Technical Information
P.O. Box 62
Oak Ridge, TN 37831

Telephone: (865)576-8401
Facsimile: (865)576-5728
E-Mail: reports@adonis.osti.gov
Online ordering: <http://www.doe.gov/bridge>

Available to the public from
U.S. Department of Commerce
National Technical Information Service
5285 Port Royal Rd
Springfield, VA 22161

Telephone: (800)553-6847
Facsimile: (703)605-6900
E-Mail: orders@ntis.fedworld.gov
Online order: <http://www.ntis.gov/ordering.htm>



SAND2002-0772
Unlimited Release
Printed April 2002

Final Report for the SEED Project (1218): “Inexpensive Chemiresistor Sensors for Real Time Ground Water Contamination Measurement”

Robert C. Hughes (PI), Chad E. Davis, and Michael L. Thomas
Microsensor Science and Technology Department
Sandia National Laboratories
P. O. Box 5800
Albuquerque, NM 87185-1425
rchughe@sandia.gov
(505) 844-8172

Abstract

This report details some proof-of-principle experiments we conducted under a small, one year (\$100K) grant from the Strategic Environmental Research and Development Program (SERDP) under the SERDP Exploratory Development (SEED) effort. Our chemiresistor technology had been developed over the last few years for detecting volatile organic compounds (VOCs) in the air, but these sensors had never been used to detect VOCs in water. In this project we tried several different configurations of the chemiresistors to find the best method for water detection. To test the effect of direct immersion of the (non-water soluble) chemiresistors in contaminated water, we constructed a fixture that allowed liquid water to pass over the chemiresistor polymer without touching the electrical leads used to measure the electrical resistance of the chemiresistor. In subsequent experiments we designed and fabricated probes that protected the chemiresistor and electronics behind GORE-TEX® membranes that allowed the vapor from the VOCs and the water to reach a submerged chemiresistor without allowing the liquids to touch the chemiresistor. We also designed a vapor flow-through system that allowed the headspace vapor from contaminated water to be forced past a dry chemiresistor array. All the methods demonstrated that VOCs in a high enough concentration in water can be detected by chemiresistors, but the last method of vapor phase exposure to a dry chemiresistor gave the fastest and most repeatable measurements of contamination. Answers to questions posed by SERDP reviewers subsequent to a presentation of this material are contained in the appendix.

Acknowledgment

We would like to thank Clifford K. Ho of the Geohydrology Department for helpful discussions on the project.

Contents

Nomenclature	7
Introduction and Background.....	8
Polymer-Based Chemiresistors	8
Chemiresistor Operation	9
Sensing in the Liquid Phase	10
Experimental Details	11
Liquid Phase Exposures	11
Vapor Phase Exposures.....	15
Results and Discussion.....	18
Liquid Phase Exposures	18
Vapor Phase Exposures.....	20
Conclusions	29
References	30
APPENDIX - Responses to Questions from SERDP Reviewers.....	31

Figures

Figure 1.	Test Cell Used for Liquid Phase Exposure of Chemiresistors.....	12
Figure 2.	Test Cell, Pump, Switch, and Water Bottles for Liquid Phase Exposures.....	13
Figure 3.	Submersible Chemiresistor Housing for Liquid Phase Exposures, (a) Without Lid and (b) Sealed and Placed Above Water Reservoir.....	14
Figure 4.	Two Configurations of Chemiresistors Used in Vapor Phase Exposures, (a) Single Ink Platform and (b) Four-Ink Chemiresistor Array.	17
Figure 5.	Equipment Used for Chemiresistor Vapor Phase Exposures.....	18
Figure 6.	Resistance/Time Plot for Liquid Phase Exposure of PEVA-40-C Chemiresistor to m-Xylene.	19
Figure 7.	Resistance/Time Plot for Liquid Phase PEVA-40-C Chemiresistor Under Vapor Phase Exposure.	21
Figure 8.	Equalized Response Plot of PDPP-40-C, PEVA-40-C, and PIB-40-C When Exposed to m-Xylene, TCE, and trans-DCE.	23
Figure 9.	Equalized Response Plot for PDPP-40-C, PEVA-40-C, and PIB-40-C When Exposed to Isooctane, Kerosene, and MTBE.	24
Figure 10.	Globe Plot for PDPP-40-C, PEVA-40-C, and PIB-40-C.....	25
Figure 11.	Equalized Response Plot for PCP-40-C, PECH-40-C, and PIB-40-C When Exposed to m-Xylene, TCE, and trans-DCE.....	26
Figure 12.	Globe Plot for PCP-40-C, PECH-40-C, and PIB-40-C.....	27

Tables

Table 1. Physical Constants for Compounds Studied.	11
Table 2. Results of the VERI Analysis for Data Presented in Figure 10.	28
Table 3. Results of the VERI Analysis for Data Presented in Figure 12.	28
Table 4. Results of VERI Analysis to Determine the Optimum Chemiresistor Array Size	29

Nomenclature

-40-C	Suffix for polymer inks, indicating percentage of total solids weight made up of graphitized carbon particles (e.g., PEVA-40-C)
DIP	dual inline package
LDRD	Laboratory Directed Research and Development
LOD	limit of detection
MTBE	methyl <i>tert</i> -butyl ether
ppb	parts per billion
ppm	parts per million
PCP	poly(chloroprene)
PDPP	poly(diphenoxyphosphazine)
PECH	poly(epichlorohydrin)
PEVA	poly(ethylene-vinyl acetate)
PIB	poly(isobutylene)
RH	relative humidity
SAW	surface acoustic wave
SEED	SERDP Exploratory Development
SERDP	Strategic Environmental Research and Development Program
SLM	standard liter per minute
trans-DCE	trans-dichloroethylene
TCE	trichloroethylene
VERI	visual-empirical region of influence
VOC	volatile organic compound
$\Delta R/R_0$	change in chemiresistor resistance due to chemical exposure divided by the baseline resistance value prior to exposure
δ	solubility parameter

Introduction and Background

The chemiresistor technology that we have developed over the last three years has been focused on the gas phase detection of many VOCs. We have learned how to fabricate arrays of different chemiresistors and how to use the patterns of response to identify individual VOCs. The statement of need for SERDP led us to consider the possibility of using chemiresistors in the liquid (aqueous) phase to detect VOC contaminants at low levels. The technical objective of this proposal is to demonstrate that our chemiresistor arrays can be packaged in such a way that they can be submerged in the aqueous phase and used to measure dissolved VOCs. To our knowledge, no one previously had used a polymeric chemiresistor for measurements in water, but considerations of the physical chemistry of partitioning of molecules between different phases led us to believe that the concept will work and that detection of contaminants in the parts per billion (ppb) to parts per million (ppm) range is possible, with the specific limit of detection depending on the individual VOC.

As a detector of organic solvents, chemiresistors may be used to locate leaks or spills of toxic chemicals and explosives, among others. As part of a system, these sensors need to be highly sensitive to small concentrations in the environment, while consuming minimal power for use in portable or remotely located devices. Such a sensor system must be able to quickly and reproducibly distinguish solvents from the ambient relative humidity, and classify the responses as a particular solvent, relative humidity, a mixture of solvents and/or humidity, or an unknown. The development of a single chemiresistor to distinguish different solvents is difficult; however, sensor arrays with several differently sensitive devices can be used to sense a wide variety of solvents. Sophisticated pattern-recognition algorithms can aid in the analysis of signals from several sensors in an array and can be used to determine the class of analyte measured [1-3]. A significant amount of research has been performed to develop sensor arrays comprised of several sensitive elements [4], which is directly applicable to our work with chemiresistor arrays.

Polymer-Based Chemiresistors

The chemiresistor is a particularly simple type of chemical sensor. Its operation relies on the change in electrical conductivity of an organic or inorganic material in response to an analyte. The selection of the material used to construct such sensor arrays depends upon the sensing task at hand. While catalytic films have been used to detect hydrogen and hydrocarbons [5], polymers are typically used to detect a broad range of solvents. Because of their versatility, polymer-based sensors are the focus of our current work on chemiresistors. The fundamental mechanism of polymer-based sensors is quite straightforward: because polymer films swell upon absorption of solvents, they exhibit measurable changes in macroscopic properties (e.g., mass, volume).

There has been significant research in developing polymer-based arrays that take advantage in these changes in macroscopic properties, using three general classes of conductive, as well as non-conductive, polymers [1-3,6]. Electrically-conductive polymers comprise two classes: (1) the “organic metals”, those organic materials that are inherently conductive due to their electronic structure, typified by polyaniline, polypyrrole, polythiophene, and polyacetylene; and

(2) composites made from conventional, insulating organic polymer matrices, loaded with conductive particles such as carbon or silver at sufficiently high levels to form continuous conductive pathways through the matrix. These types of composite materials have long been used as positive-temperature-coefficient resistors in electronics, and even as gas phase chemical sensors for nearly 20 years. The composite film resistance depends strongly on the concentration of the carbon or metal and on temperature [7-11]. Appropriately prepared films from both of these categories allow straightforward direct current resistance measurements of film properties, without large power requirements or complex circuits. Unfortunately, for both classes of conductive polymer materials, fabrication of films with reproducible behavior is often difficult. The third class of polymers, non-conducting polymer films, is typically fabricated from a single component of a conventional polymer. This type of polymer film is often much easier to make in highly reproducible form, but are not suitable for electrical resistance measurements essential to the operation of a chemiresistor. Although either of the two types of electrically conductive polymers would be functional in the chemiresistor application, the second, or conductive particle-loaded polymers, have been the focus of our work to date, as these composite films can be made of any polymer with varied conductive particle concentration. Therefore, chemical sensitivity remains the driving force for chemiresistor material selection.

The actual polymer selection process was facilitated by drawing on results of testing from other types of polymer-based sensors used for solvent detection. For example, surface acoustic wave (SAW) devices, which respond to changes in surface mass and film mechanical properties, can be used with completely insulating materials or can also be used with any of the types of conductive materials, provided that the conductive materials are patterned so as not to short out the transducers. These devices are generally very sensitive, and the absorption of many solvents by polymers in SAW devices has been studied in great detail [3,12,13]. Knowledge gleaned from work with the SAW devices, which require complicated high-frequency circuitry, was used to advance our research with the chemiresistors, which, by comparison, serve as a simple, inexpensive, and easily fabricated alternative for sensor arrays.

Chemiresistor Operation

If a polymer/conductive particle composite increases in volume by thermal expansion or by swelling from absorbing a chemical, the electrical resistance increases due to a breaking of some of the conductive pathways through the film. The expansion can produce large increases in resistance if the polymer volume is changed close to the percolation threshold [10-11,14]. This threshold concentration has been found to be between 20 and 40% by volume of the conductive particles. The response of these composite films to different solvents depends on the particular solvent-polymer interaction, while the conductive particles only report the degree of swelling [7,8]. Such materials have been modeled as a network of resistors and diodes, where resistors represent the conductive network of carbon particles and diodes represent the polymer-filled dielectric gaps between the particles [9].

The degree of swelling of a particular polymer is related to its solubility parameter (δ) and the solubility parameter of the solvent. The solubility parameter is used to describe the free energy of mixing of non-polar, non-associating fluids, and can be extended to other solvents and to polymers, so long as the interaction process is not exothermic. Two solvents that have identical

values of δ will form ideal solutions and will have almost zero heat (enthalpy) of mixing. Such ideal solutions of two liquids follow Raoult's law: the vapor pressure of each of the solvents is proportional to the mole fraction of the solvent in the liquid phase. The amount of solvent-induced polymer swelling depends in turn on the partitioning of the solvent vapor into the polymer film [7,8].

The solubility parameter and the idea of partitioning of the solvent between two phases have already been studied for determining the relative responses of gas sensor arrays [2,7,8,12,15]. Since it is unlikely that a specific polymer will be sensitive to only one solvent (every polymer absorbs a number of solvents having similar solubility parameter values), an array of sensors is an effective means to discriminate against interfering vapors. A common and obvious source of interference is relative humidity in the ambient environment. Water vapor has been found to change the relative sensitivity of certain polymers to solvent vapors and the patterns of responses obtained from arrays containing those polymers [6]. To build a sensor array that is capable of identifying the maximum number of analytes, the array should contain several different sensors that are as chemically varied as possible, with at least one sensor having significant sensitivity to relative humidity.

Sensing in the Liquid Phase

A chemiresistor fabricated from a non-polar polymer like poly(isobutylene) (PIB) gives very little response to water vapor, even 100% relative humidity. This gives us confidence that placing the sensor in liquid water will not cause any significant problems. Of course the exposed part of the electrodes and the wirebonds to the sensors must be encapsulated so that liquid water, particularly water with ions in it, does not contact the metal electrodes (currents flowing through the water would be confused with the current flowing through the chemiresistor). VOCs that are almost insoluble in water will partition out of the water into a polymer that has a similar solubility parameter, allowing for good detection capabilities. A general prediction about these detection capabilities can be established based on past experience with chemiresistors in the vapor phase, and using information from Henry's law, which tells us about the partitioning of a VOC between the water phase and the air phase. For example, m-xylene has a solubility of 1.7 moles per cubic meter in water at 25°C. This corresponds to 28 ppm and this is the maximum amount of m-xylene that can be in the water at one atmosphere, even if liquid m-xylene is also present. The vapor pressure of liquid m-xylene at 25°C is 1.1 kPa. Henry's law states that the amount of m-xylene in the liquid phase is directly proportional to the vapor-phase pressure. Thus a contamination of 310 ppb in the water phase has, at equilibrium, a gas phase vapor pressure of 0.011 kPa, 100 times smaller than the saturated vapor pressure (corresponding to about 100 ppm in the gas phase).

There are large tables of data giving the Henry's law constants for chemicals of environmental interest [16]. Figure 1 of that paper is particularly interesting for the application of chemiresistors to the problem of monitoring VOC contaminants. It shows a log-log plot of the solubility (in moles per cubic meter, at the saturated vapor pressure) versus the saturated vapor pressure of a very large number of VOCs. Over 13 decades of vapor pressure values are shown, and 10 decades of solubility values. In our studies we have found that by picking the best polymer for use as a chemiresistor to detect a particular analyte, we can detect concentrations

that are about 1000 times lower than the saturated vapor pressure of any particular VOC. This makes it appear that the sensors are more sensitive to VOCs with very low saturated vapor pressures when the concentrations are given in terms of ppm or ppb. Because Henry's law is linear over the whole concentration range, we can predict from the solubilities of given VOCs what the detection limit will be: about 1000 times lower than the solubility at saturation. From the log-log plot we can see that many compounds of interest have solubilities of 0.1 mol per cubic meter or less, which corresponds to 2 ppm or less. This means that we predict that we will be able to detect ppb levels with a chemiresistor immersed in the water phase.

Table 1. Physical Constants for Compounds Studied¹.

Compound	Vapor Pressure (torr)	Solubility (ppm, mole/mole, 25°C)	Henry's Law Constant (ppm vapor/ppm mole/mole, 25°C)
MTBE ²	245	1e4	32
m-xylene	7	28	328
TCE	68	152	588
trans-DCE	331	1200	364
Dodecane (Kerosene)	0.12	3.4e-4	5e5
Isooctane(2,2,4 trimethylpentane)	50	0.38	170,000

¹Mackay, D; Shiu, W. Y. *J. Phys. Chem. Ref. Data*, **1981**, *10*, 1175.

²Merck Index, 12 edition, compound 6111 (1996), Merck Research Labs, Whitehouse Station, NJ

Looking at the solubility column in Table 1, we can estimate the lowest detectable concentration on the best chemiresistor for the compounds we studied by dividing by 1000. The units here are moles of analyte to moles of water. Many people use concentration in grams of analyte per gram of water; to get that you multiply by the ratio of the molecular weight of the analyte to water (18 grams per mole). The actual limit of detection (LOD) will depend on the baseline stability of the chemiresistor; some data will be presented in the results section.

Experimental Details

Experiments for detection of VOCs in water were performed both in the liquid phase by immersing the chemiresistors, and in the vapor phase by exposing the chemiresistors to a gas stream that approximates conditions in the headspace above a contaminated water source. Details for experiments in both phases are contained below.

Liquid Phase Exposures

Two configurations of chemiresistor were used in the liquid phase exposures. One involved a large chemiresistor of poly(ethylene-vinyl acetate) (PEVA) formed on an array of platinum

electrodes originally designed for planar electrochemical experiments. When placed in the fixture shown in Figure 1, liquid can be pumped across the surface of the chemiresistor without liquid touching the electrical leads to the chemiresistor. Spring-loaded pogo pins are used to make the electrical connections from the internal sensor electrodes to the external wiring, and an O-ring prevents the liquid from reaching the bonding pads or the pogo pins. Figure 2 shows the Rainin RP-1 peristaltic pump and associated apparatus used for liquid phase exposures, with the bottles used to supply contaminated water and clean water to the sensor. In the foreground is the valve used to switch between solution bottles. It can be seen that only a short length of tubing needs to be purged when switching from one bottle to the other.

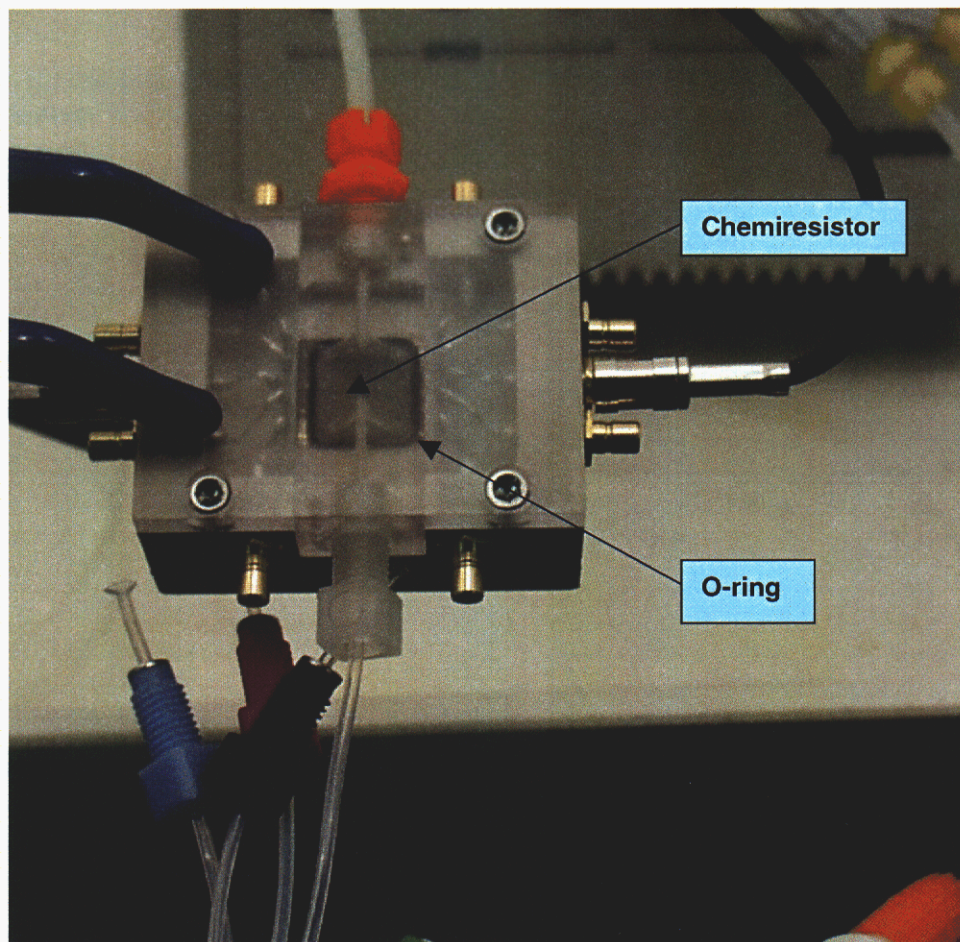


Figure 1. Test Cell Used for Liquid Phase Exposure of Chemiresistors. Water is injected directly on the surface of the chemiresistor polymer, coated on an array of platinum electrodes and bounded by the O-ring. The O-ring prevents water from contacting the electrical connections in the sensor housing.

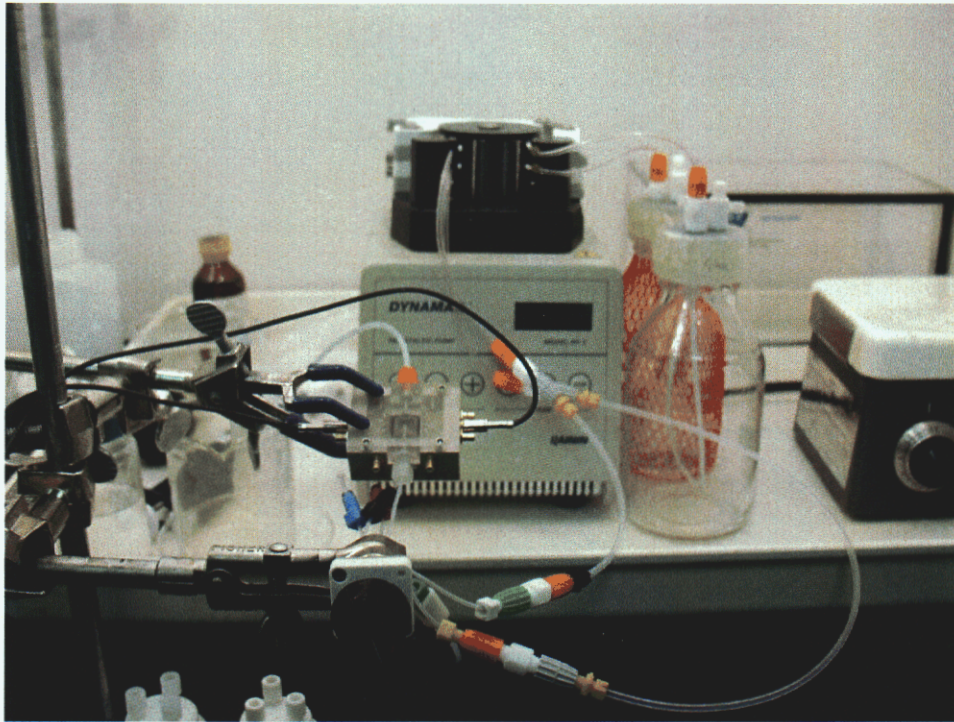


Figure 2. Test Cell, Pump, Switch, and Water Bottles for Liquid Phase Exposures.

The flow injection apparatus includes separate bottles that contain clean and contaminated water supplies for chemiresistor exposure.

The second chemiresistor configuration used for liquid phase exposures consisted of an array of four chemiresistors traditionally used for vapor phase exposures in a waterproof probe with simple electronics for reading one chemiresistor and the on-chip temperature sensor (see more detailed discussion of chemiresistor array platforms in the Experimental Design subsection entitled “Vapor Phase Exposures”). The chemiresistor array was exposed to VOC vapors through a GORE-TEX® membrane so that liquid water did not touch the chemiresistor polymer. Figure 3 shows both the open and closed version of this sensor system. A custom-made gasket prevented water from leaking into the sensor housing. The apparatus for containing the contaminated water was fitted with a thermocouple for water temperature measurements, a port for sparging through a tube with a diffuser on the end (under water), a magnetic stir bar, a port for the chemiresistor probe, and a port for a ToxiRAE PGM-30 handheld photo-ionization detector used to provide an independent reading of VOC concentration in the headspace (not in the water). The sparge tube can also be used to introduce a known concentration of VOC from our gas test bed flow controllers. VOC can also be introduced by injection directly from a syringe into the stirred water, in which case the VOC was usually dissolved in methanol as an intermediary to facilitate complete mixing in the liquid water.



Figure 3. Submersible Chemiresistor Housing for Liquid Phase Exposures, (a) Without Lid and (b) Sealed and Placed Above Water Reservoir.

The top picture (a) shows the internal circuitry for monitoring resistance and temperature measurements of the chemiresistor array, noted as device “A28”. The electronics are self-contained, so that a buffered voltage signal comes out on a waterproof cable. The voltage is proportional to the chemiresistor resistance. The bottom picture (b) shows the sensor housing prior to submersion in the water reservoir. The housing lid is fitted with a GORE-TEX® membrane to allow water and VOC vapors through, while excluding liquid water. The water reservoir accommodates a stir bar for mixing, a thermocouple for water temperature measurement, and an access port for a commercial handheld photo-ionization detector for confirming VOC concentrations in the headspace vapor.

Vapor Phase Exposures

For the vapor phase exposures, two types of silicon electrode platforms, fabricated at Sandia, were used in this study. Figure 4 shows close-up pictures of these two types of chemiresistors. The first type of platform (shown in Figure 4a), a single-ink chemiresistor platform, consists of four interdigitated platinum traces with a titanium adhesion layer on an insulating layer of silicon nitride. Each trace is connected to a large pad for ease of electrical connections. Inner traces are separated by a 50 μm gap. As shown in Figure 4a, the single chemiresistor chip requires no wire bonds. Pogo pins inside the chip housing are used to make contact so chips can be changed out quickly. The fixture has small ports for flowing vapor across the chip and an O-ring seal.

The second type of platform (shown in Figure 4b), a four-ink chemiresistor array platform, incorporates four of the single-ink chemiresistor arrangements, along with a platinum trace temperature sensor and two platinum heater bars that may be used to control the temperature of the device. For these devices, both 50 and 100 μm inner trace spacing was used. As seen in Figure 4b, the platinum temperature sensor is in the middle of the chip and the heater bars are on the two ends. Each different ink is placed on the four electrode traces so a four terminal resistance measurement can be made. For this platform, the wire bonds to the dual inline package (DIP) can also be seen in Figure 4b.

“Ink” solutions deposited on the electrode platforms consist of a polymer in solvent, mixed with 20 – 30-nm graphitized carbon particles (obtained from Polysciences, Inc.). The polymers used in this study include poly(chloroprene) (PCP), poly(diphenoxyphosphazine) (PDPP), poly(epichlorohydrin) (PECH), PEVA, and PIB. All polymers were obtained from either Polysciences, Inc., Scientific Polymer Products, Inc., or Aldrich Chemical Company. Solvents include chlorobenzene, chloroform, and water. Ink preparation typically involved 0.06 grams of polymer and 0.04 grams of carbon particles in 5 mL of solvent. (Inks are referred to by name followed by “-40-C” to note that carbon particles make up forty weight percent of the solids.) Inks were subjected to sonication from a point ultrasonic source, using 15 half-second pulses separated by one-second rest periods. Ink deposition was performed with a filtered syringe on single-ink platforms, and with an Asymtek Century Series C-708 automated fluid dispensing system on the smaller four-ink array platforms. In three cases, the polymer ink included a surfactant to help promote carbon particle dispersion, and enhance chemiresistor response stability. The selection of the particular ink polymer-surfactant combinations were based on initial screening data, and included PEVA-40-C with Spurso (purchased from OMG Americas, Inc.), PIB-40-C with Polyglycol EP-530 (purchased from The Dow Chemical Company), and PDPP-40-C with Ralufon DS (purchased from Raschig AG).

Chemiresistors are exposed to chemical analytes in the vapor phase through the use of a nitrogen gas stream passing through gas washing bottles filled with the analyte of interest. A ceramic frit at the bottom of the bottle allows the nitrogen gas to be broken into a fine stream of bubbles. Intimate contact between the liquid analyte and the gas bubbles allows the gas stream to exit the bottle in a saturated condition. Analyte concentration is controlled by a set of mass flow controllers. Analytes used in this experiment include isooctane, kerosene, methyl *tert*-butyl ether (MTBE), trans-dichloroethylene (trans-DCE), trichloroethylene (TCE), and m-xylene. For vapor phase exposures, once analyte concentrations are set through the use of the gas washing bottles

and the mass flow controllers, the gas stream was sent through a final gas washing bottle filled with water to provide a background of 100% relative humidity.

For vapor phase exposures, the chemiresistors were placed in a temperature-controlled environment to try to ensure that the device temperature did not drop below the vapor condensation temperature. Figure 5 shows the inside of the oven used for temperature control purposes. The oven is inside a walk-in hood so toxic vapors can be tested and safely controlled. Inside the oven are the test cells for both the four-ink chemiresistor array and the single-ink chemiresistor platform. The triangular-shaped fixture in the upper left corner of the picture holds a chemiresistor array, and the long stainless steel cell in the bottom of the picture can hold up to eleven single-ink platforms. By simply connecting the test cells in series, many sensors can be exposed at once to the same vapor stream. As shown in Figure 5, the test apparatus is set up to collect data from the four chemiresistors on the array in the triangle cell and from six single-ink platforms in the stainless steel cell. Tubing connects the outlet of the stainless steel cell to the inlet of the triangle cell. The copper coil upstream of the stainless steel cell, seen in the upper center portion of the picture, allows the vapor stream to equilibrate with the oven temperature before being directed to the chemiresistors.

For all experiments, electrical resistances and thermocouple measurements were taken using a Hewlett Packard 34970A digital multimeter and recorded by a LabVIEW® program on an Apple Macintosh® computer.

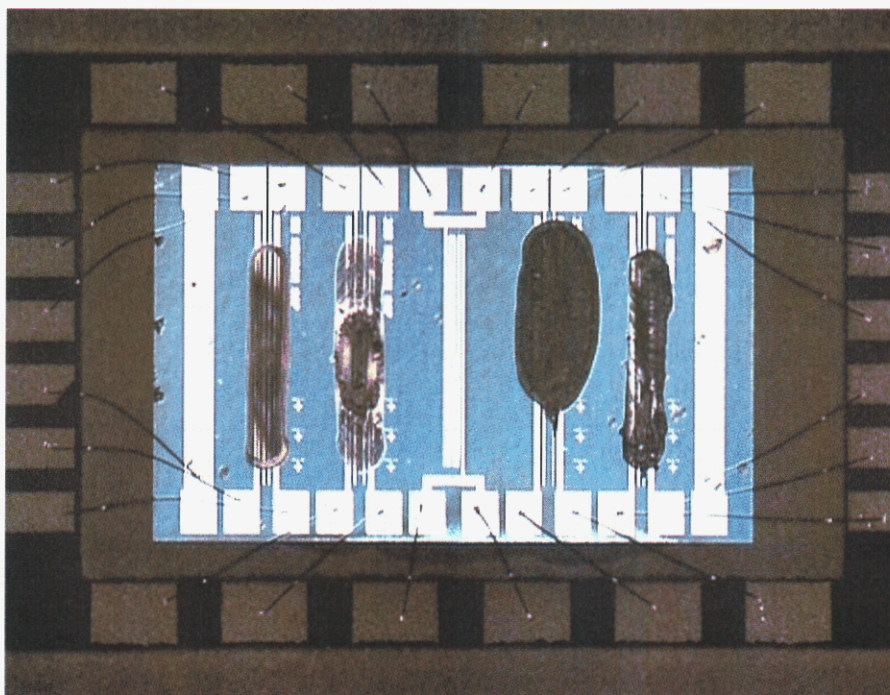
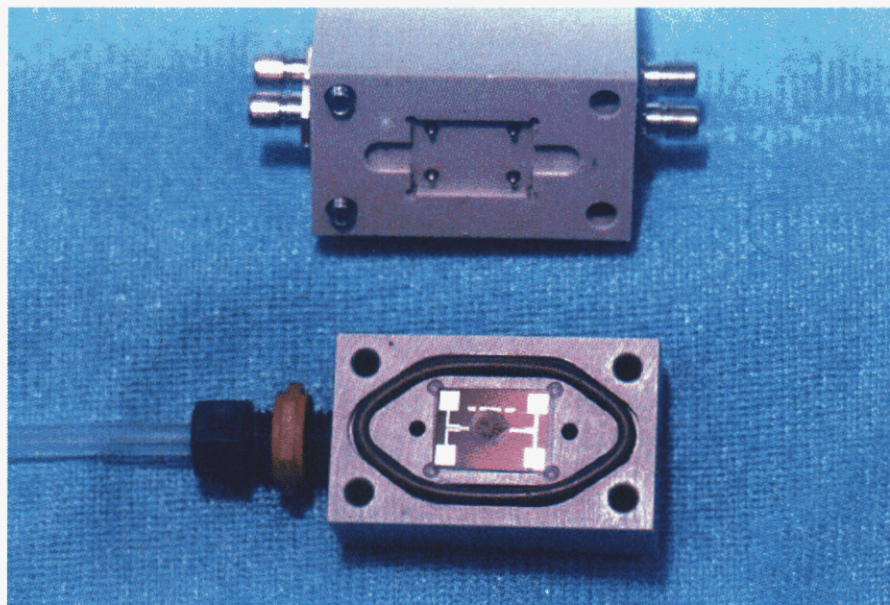


Figure 4. Two Configurations of Chemiresistors Used in Vapor Phase Exposures, (a) Single Ink Platform and (b) Four-Ink Chemiresistor Array.

The upper picture (a) shows a fixture for a single chemiresistor chip requiring no wire bonds. Pogo pins are used to make electrical contact so chips can be changed out quickly. The fixture has small ports for flowing vapor across the chip, and is fitted with an O-ring seal. In the lower picture (b), the integrated platinum-wire temperature sensor is seen in the middle of the array platform, and the heater bars are on the left and right ends of the platform. The chip has dimensions of about 0.8 cm by 0.3 cm. Each ink is placed on the four electrode traces so a four terminal resistance measurement can be made. The wire bonds to the DIP package can also be seen.

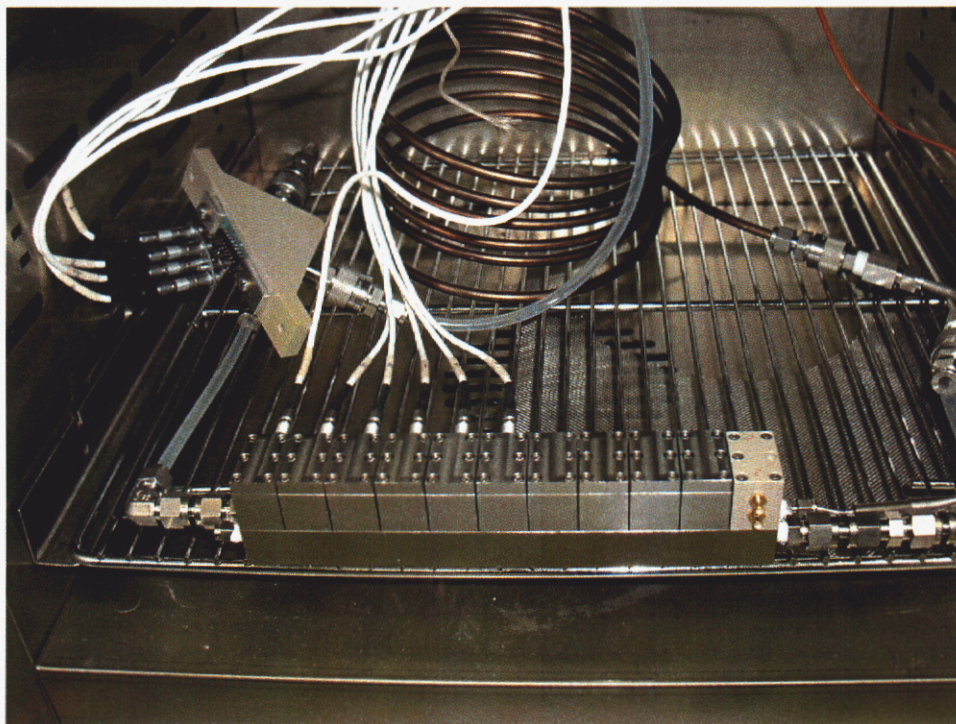


Figure 5. Equipment Used for Chemiresistor Vapor Phase Exposures.

The picture shows the inside of an oven used for temperature control in vapor phase exposures. The triangular-shaped cell in the upper left quadrant of the picture holds one chemiresistor array. The long, narrow stainless steel cell in the lower half of the picture can hold up to eleven single-ink chemiresistor platforms. In this particular configuration, using both the triangle cell and the stainless steel cell, one chemiresistor array and six single-ink platforms can be tested at a single time, as limited by the data acquisition device.

Results and Discussion

Liquid Phase Exposures

A number of experiments were performed with the chemiresistor and apparatus shown in Figures 1 and 2. Figure 6 shows a plot of resistance as a function of time obtained through a liquid phase exposure of PEVA-40-C to water contaminated by m-xylene. The flow rate was set at approximately 1.8 mL per minute, and the concentration of m-xylene in the contaminated water bottle was fixed at 3 ppm (mole/mole) by a constant flow of dilute (10%) m-xylene vapor through the diffuser in the water bottle. The diffuser ensures that after a few minutes the concentration of xylene in the water is in equilibrium with the vapor concentration; the water concentration is computed from the Henry's Law constant given in Table 1. The switch from the clean bottle to the contaminated bottle occurs at the point labeled "1". The signal is seen almost immediately, but takes a long time to reach steady state. At "2" the flow is switched back to the clean bottle. At "3" the flow is switched back to the contaminated bottle, but the pump speed is set at the "prime" speed, providing the maximum flow rate for this particular pump (approximately 9.1 mL per minute). The response is clearly faster and this expose and purge

cycle is repeated at the high speed at “4”. At “5” the chemiresistor was exposed twice to 1 ppm m-xylene while maintaining the same faster flow rate, and the lower concentration is matched by a corresponding lower signal.

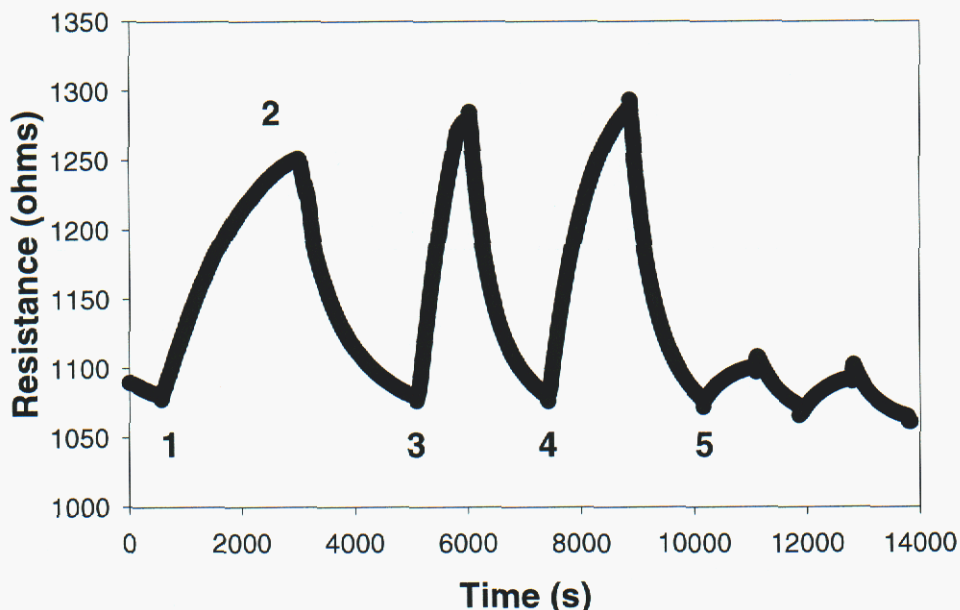


Figure 6. Resistance/Time Plot for Liquid Phase Exposure of PEVA-40-C Chemiresistor to m-Xylene.

At point (1), the flow was switched from the bottle of clean water to the bottle of water containing 3 ppm dissolved m-xylene. At (2) the flow was switched back to clean water, allowing the chemiresistor to recover. At point (3), a faster pumping speed allowed the chemiresistor to show a faster response to the same concentration. The exposure at the faster pumping rate was repeated at (4). Two successive exposures to 1 ppm m-xylene in water are shown at (5).

For the purposes of comparison, the same chemiresistor was calibrated by passing known vapor concentrations across it in the same fixture (see the following section on vapor phase exposure results). Signals from contaminated water touching the chemiresistor polymer directly gave resistance changes (signals) similar in size to the vapor exposures, but the sensor was slower to reach a steady state value. The slow response is probably due to the slow transfer of m-xylene molecules out of the water into the polymer. The diffusion constant of m-xylene in water is approximately four orders of magnitude lower than in air, and the low concentration in the water means that the boundary layer next to the polymer is quickly depleted of m-xylene. Faster pumping seems to replenish the boundary layer to give a faster response.

Beyond a slower response time, there were other problems we encountered with allowing the liquid water to touch the chemiresistor polymer in the liquid phase experiments. Long exposure (weeks) in two cases led to delamination of the polymer from the electrodes even though the polymers are highly hydrophobic (both PIB-40-C and PEVA-40-C). Because of slower response and short lifetimes through allowing water to contact the chemiresistor materials, efforts then shifted to liquid phase exposures using the submersible housing shown in Figure 3 that would protect the chemiresistor from liquid water while allowing VOC and water vapors to reach the

chemiresistor through the GORE-TEX® membrane. In our experiments, the GORE-TEX® membrane successfully protected the entire housing from water intrusion, and the chemiresistor inside was able to detect both VOC and water vapors. To keep the electronics inside the housing from being damaged by the potential effects of liquid water, the chemiresistor chip heater bars (see Figure 4) can be used to maintain the chip above the water condensation temperature of the vapor. Based on the initial success of our experiments with the submersible housing, all our subsequent experiments focused on vapor phase exposures under conditions of 100% relative humidity. Data from these experiments could then be applied either to a dry sensor placed in the headspace of a contaminated water supply, or to a “wet” sensor submerged in the liquid phase (with sensors kept dry by a hydrophobic membrane) that simply detects concentrations in the small headspace of the sensor housing.

Vapor Phase Exposures

A first example of the chemiresistor responses from vapor phase exposures of m-xylene at different concentrations under both dry and 100% relative humidity (RH) conditions is shown in Figure 7. This chemiresistor is in fact the same one shown in Figure 1, only with vapor forced across it instead of liquid water. The dry exposures (dashed line) show good repeatability of the same concentration of m-xylene and a fast response both to exposure and removal of the analyte. The water headspace responses, shown by the solid line in Figure 7, were obtained by forcing the same vapor concentration through a water-filled gas washing bottle with about 500 mL of water in it. The offset in response for the 100% relative humidity data when compared with the dry data is caused by loss of m-xylene from the gas feed into the water-filled gas washing bottle at the start of the exposure, and by the time required to remove the m-xylene from the water by sparging on the purge side after the end of the exposure. In fact this experiment gives a real-time measurement of the sparging of the contaminated water. In other experiments we showed the expected behavior of the sparging on the flow rate; a 10 times lower flow rate (0.1 standard liter per minute (SLM) vs. 1 SLM) gave about 10 times slower sparging of the m-xylene. An increase in the volume of water in the gas washing bottle also gave the expected longer time responses.

As seen through the slow sparging experiments, even a low flow rate quickly brings the chemiresistor into equilibrium with the headspace concentration of VOC, and would be a good way of sampling in the field (a hand pump would be sufficient for the very small dead space volumes that can be fabricated for these miniature sensors). The water vapor by itself does give some signal on all the chemiresistors we have studied. This “baseline” or offset is affected by the water temperature, the real RH, and the sensor chip temperature. There is always some unpredictable baseline drift associated with the RH; some can be seen in Figure 7. In experiments performed for another program we have shown that maintaining the sensor chip temperature a few degrees above the liquid water temperature decreases the baseline drift and offset problems.

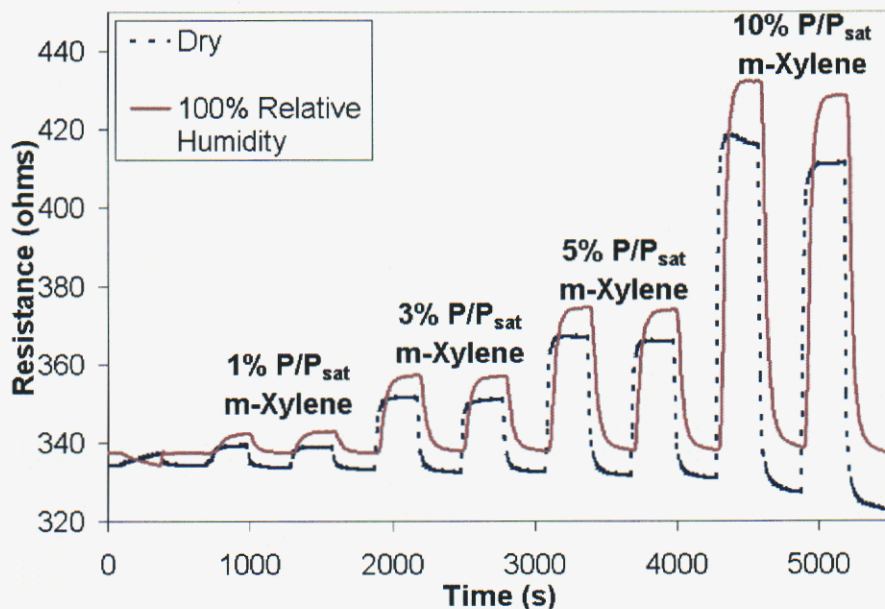


Figure 7. Resistance/Time Plot for Liquid Phase PEVA-40-C Chemiresistor Under Vapor Phase Exposure.

The plot shows the response of an individual chemiresistor to m-xylene vapor at different concentrations, expressed as the percentage of saturated vapor pressure at 21°C. A concentration of 10% P/P_{sat} corresponds to about 1000 ppm in the vapor phase and 3 ppm in the water phase. Two sequences of vapor pulses are shown: one with dry nitrogen as the carrier gas for the m-xylene, and one with the m-xylene-loaded nitrogen stream passing through a water-filled gas washing bottle to provide potential interference from 100% relative humidity. Inclusion of humidity simulates the headspace of a contaminated water sample. The graph shows that the sensor has no difficulty operating in humid conditions. The slight time offset and slope differences between the exposure peaks for the dry condition and 100% relative humidity condition are due to the loading and sparging of m-xylene in the water-filled gas washing bottle.

Additional headspace exposure experiments were performed using one four-ink chemiresistor array and six single-ink chemiresistor platforms, as shown in Figure 5. All ten chemiresistors were exposed simultaneously to an individual analyte in concentrations of 1, 3, 5, and 10 percent of the saturated vapor pressure at room temperature. An exposure at a given concentration was maintained for ten minutes across the chemiresistors before purging the system with a clean nitrogen stream for ten minutes. Consistency in chemiresistor response was noted by repeating each concentration four times before proceeding to the next concentration. Chemiresistor response to an exposure was noted by recording the changes in two-wire electrical resistance across two of the four electrodes, and was quantified as a ratio of the change in resistance caused by chemical exposure to the baseline resistance prior to the exposure (referred to as $\Delta R/R_0$).

Data from the best five chemiresistors are presented in Figures 8 through 12. Figures 8, 9, and 11 show equalized response values for the exposure of three chemiresistors to a series of three analytes, where equalized responses are calculated by taking all the values of $\Delta R/R_0$ for a given chemiresistor and dividing by the largest single $\Delta R/R_0$ value from all tested analytes for that

particular chemiresistor. Figures 10 and 12 show three-dimensional “globe” plots used for simple pattern recognition purposes. In each “globe” plot, data from three different chemiresistors are presented on a set of orthogonal axes, with each exposure of an analyte at a given concentration represented by a single marker on the surface of one-eighth of a unit sphere. The coordinates of the point on the sphere are based on the normalized response values for each of the three polymers on the three axes. The normalized coordinate values for a single analyte exposure are calculated by dividing each of the three equalized values from the three chemiresistors, in turn, by the square root of the sum of the squares of the three equalized responses:

$$N_i = \frac{E_i}{\sqrt{E_1^2 + E_2^2 + E_3^2}}$$

where N_i is the normalized coordinate value for chemiresistor i , E_i is the equalized response for chemiresistor i , and $i = 1, 2, \text{ or } 3$ [17].

The first of the equalized data plots, Figure 8, shows the data for polymers PEVA-40-C, PDPP-40-C, and PIB-40-C when exposed to *m*-xylene, TCE, and *trans*-DCE. Each chemiresistor shows sensitivity to changes in concentration for a given analyte, and even shows some slight differences from analyte to analyte. For all three polymers, the response to TCE is greater than the response to *m*-xylene, and the response to *trans*-DCE is even slightly greater than the response to TCE. It is also important to notice that the relative magnitude of response across the three sensors is essentially the same for all exposures.

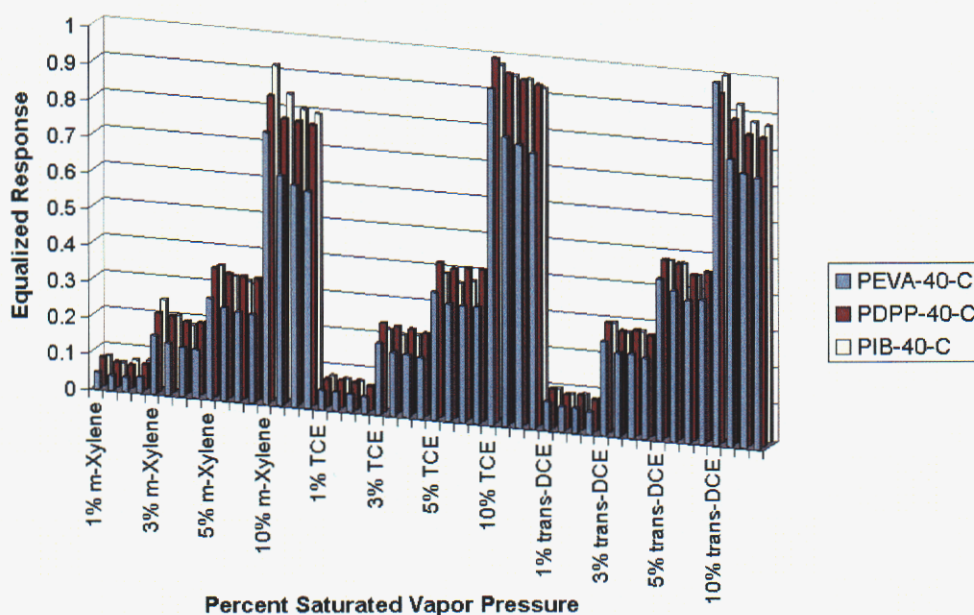


Figure 8. Equalized Response Plot of PDPP-40-C, PEVA-40-C, and PIB-40-C When Exposed to m-Xylene, TCE, and trans-DCE.

Chemiresistors were exposed to the analytes in concentrations of 1, 3, 5, and 10 percent of the saturated vapor pressure at room temperature. Chemical analyte response values are calculated by taking the ratio of the increase in resistance due to chemical exposure to the baseline resistance prior to exposure.

Equalized responses are presented by dividing all calculated response values for a given polymer by the largest response from all tested analytes for that polymer. The response of a chemiresistor to the presence of an analyte can be seen for each of the three polymers. In this figure, each of the three polymers shows a similar relative magnitude of response to all three analytes in any concentration, with PEVA-40-C responding less than both PDPP-40-C and PIB-40-C, which show fairly comparable responses.

Figure 9 shows equalized data for the same three chemiresistors when exposed to isooctane, kerosene, and MTBE. As in Figure 8, the three chemiresistors show individual sensitivity to changes in concentration. Unlike Figure 8, however, these chemiresistors also show differences in the relative responses to the three analytes. The PIB-40-C shows the strongest response of the three chemiresistors to both isooctane and kerosene, while the PDPP-40-C shows the strongest response to MTBE. The PEVA-40-C, while maintaining a fairly consistent response to all three analytes, shows a stronger relative response to kerosene than to isooctane, when compared with the other two chemiresistors.

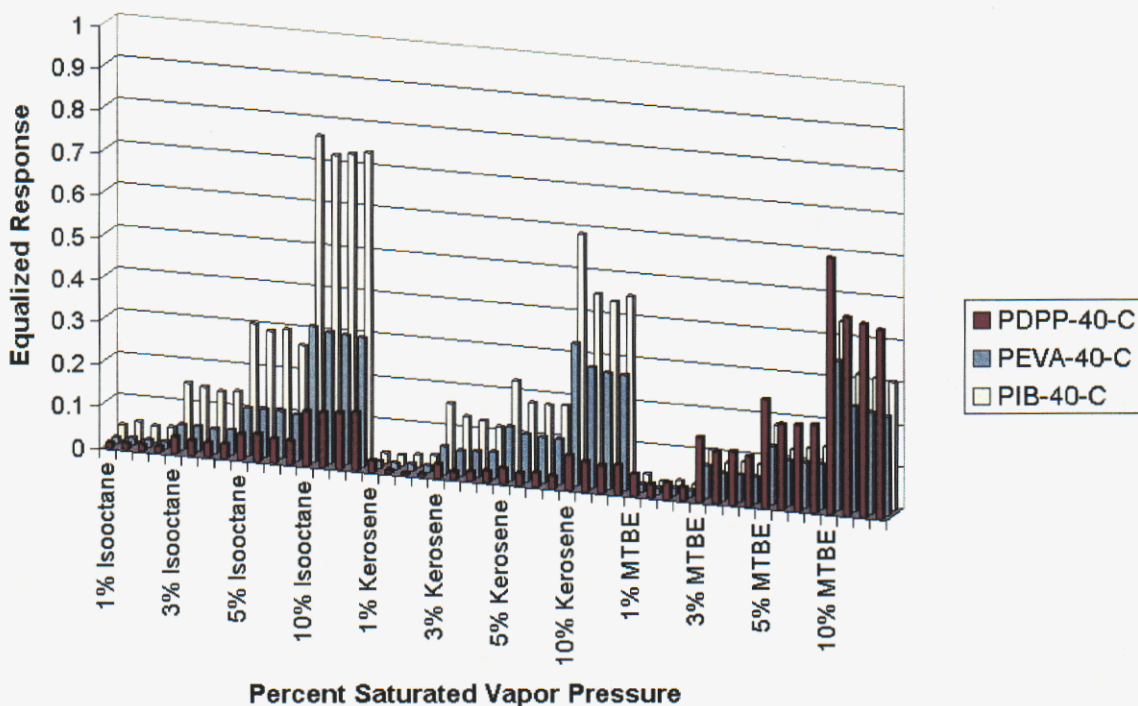


Figure 9. Equalized Response Plot for PDPP-40-C, PEVA-40-C, and PIB-40-C When Exposed to Isooctane, Kerosene, and MTBE.

Each chemiresistor responds not only with changes in concentration, but also shows a different response to different analytes. In this figure, PIB-40-C clearly shows the strongest response of all three chemiresistors for both isooctane and kerosene, while PDPP-40-C shows the strongest response for MTBE. PEVA-40-C, with a fairly consistent equalized response to all three analytes, shows a greater relative response to kerosene than to isooctane when compared with the other two chemiresistors.

The information presented in Figures 8 and 9 can then be captured and presented with some elements of pattern recognition through the “globe” plot in Figure 10. As noted for Figure 8, these three chemiresistors show fairly consistent relative magnitudes of response for TCE, trans-DCE, and m-xylene. This consistency is seen in Figure 10 through a close grouping of the data points for these three analytes near the middle of the plot. The comparable relative equalized values, when taken in a ratio, as in the previous equation, result in similar normalized coordinate values for all three sensors. The polymer-based sensitivities seen in Figure 9 for isooctane, kerosene, and MTBE, however, can be seen through the separation of these three analytes in Figure 10. The strong response to both isooctane and kerosene from PIB-40-C places the data points for both analytes near the top of the plot, corresponding to high values on the PIB-40-C axis. Similarly, the strong response from PDPP-40-C places the data points for MTBE lower on the globe plot, in a region corresponding to higher values on the PDPP-40-C axis. Although the equalized response of the PEVA-40-C is not as large as the equalized response from the PIB-40-C, the stronger relative magnitude of response from the PEVA-40-C to kerosene when compared with isooctane shifts the data points for this analyte to the left, corresponding to higher values on the PEVA-40-C axis. However, while this globe plot might make it possible to identify MTBE, isooctane, and kerosene from chemiresistor data, it would be

difficult, if not impossible, to tell the difference between TCE, trans-DCE, and m-xylene. For this purpose, data from additional chemiresistors is necessary to discriminate among these three analytes.

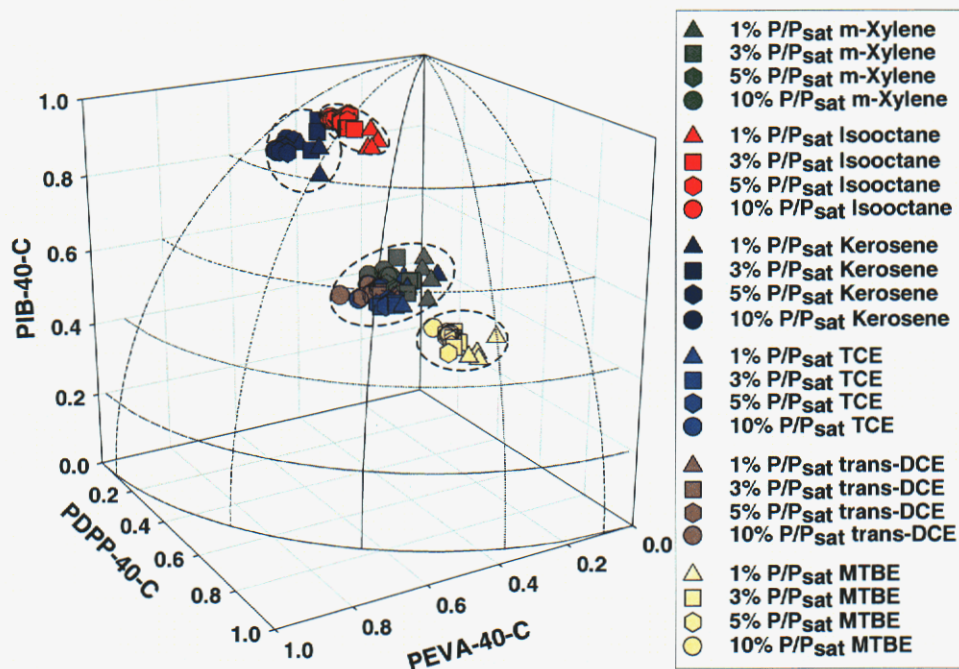


Figure 10. Globe Plot for PDPP-40-C, PEVA-40-C, and PIB-40-C.

Equalized responses from each of the three polymers are converted to globe plot coordinates by dividing each polymer's equalized response by the square root of the sum of the squares of the three responses. As noted in Figure 8, all three polymers show responses of comparable magnitude for TCE, trans-DCE, and m-xylene. In this globe plot, this similarity of relative magnitudes is shown by a clustering of points near the middle of the plot for these three analytes. As noted in Figure 9, relative magnitude of response for isooctane, kerosene, and MTBE do show polymer-based differences, shown in this plot as a different region for each analyte. Because MTBE shows the strongest response out of the three chemiresistors from PDPP-40-C, the MTBE data points are grouped at a point corresponding to a higher value on the axis representing PDPP-40-C responses. Similarly, data points for both isooctane and kerosene are grouped around values that correspond to higher values on the axis representing PIB-40-C responses. Also, as noted in Figure 9, the larger relative magnitude of response from PEVA-40-C to kerosene when compared with isooctane places the kerosene data points around values that correspond to higher values on the axis representing PEVA-40-C responses.

Figure 11 shows the equalized data for PCP-40-C and PECH-40-C in combination with the PIB-40-C used in Figures 8 through 10. As in Figure 8, these three chemiresistors are exposed to m-xylene, TCE, and trans-DCE. However, unlike Figure 8, the relative magnitude of response for these three chemiresistors to these three analytes begins to show some analyte separation qualities, similar to that of Figure 9. In Figure 11, PECH-40-C shows the strongest response to m-xylene, while PIB-40-C shows the strongest response to TCE. All three chemiresistors show

comparable and strong responses to trans-DCE. Of particular interest and even greater usefulness is the fact that PCP-40-C has such a relatively small response to m-xylene.

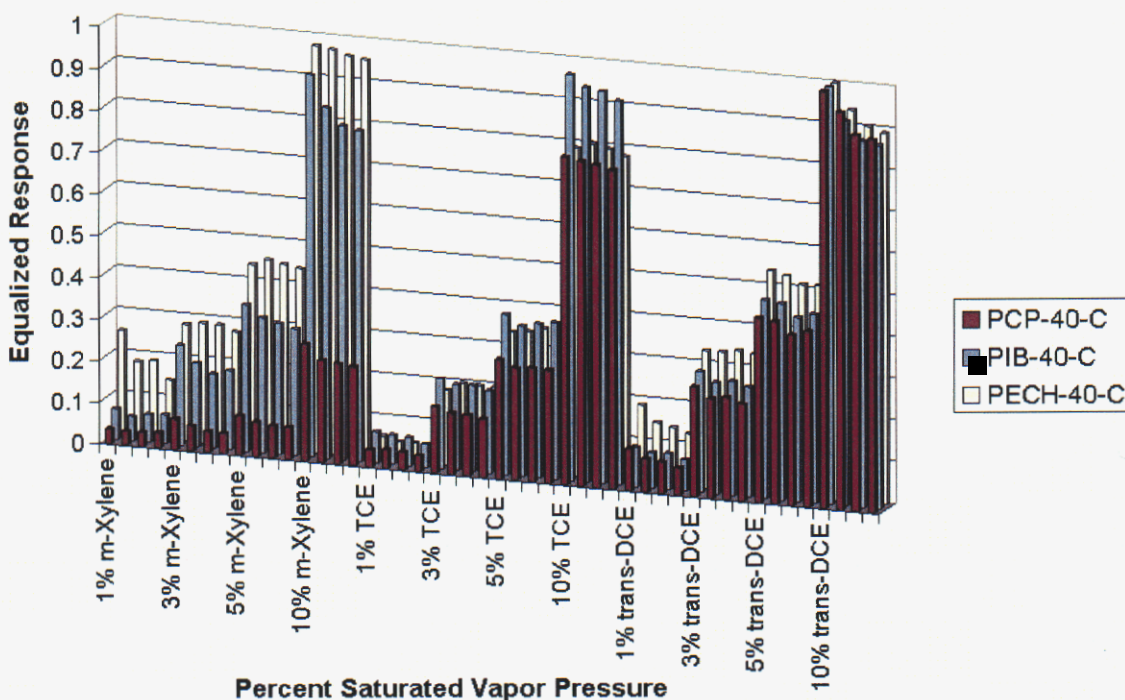


Figure 11. Equalized Response Plot for PCP-40-C, PECH-40-C, and PIB-40-C When Exposed to m-Xylene, TCE, and trans-DCE.

As in Figure 8, the three chemiresistors show a different response based on changes in analyte concentration. Unlike Figure 8, however, the three chemiresistors show significantly different relative magnitudes of response for the three different analytes. PECH-40-C shows a strong response to both m-xylene and trans-DCE, with a more moderate response to TCE, while PIB-40-C shows a fairly strong response to all three analytes, and PCP-40-C shows a small response to m-xylene, a more moderate response to TCE, and a strong response to trans-DCE. On a relative scale, PECH-40-C shows the strongest response for m-xylene, PIB-40-C shows the strongest response for TCE, and all three chemiresistors show comparable strong responses for trans-DCE.

In the “globe” plot of Figure 12, the responses of the PCP-40-C, PECH-40-C, and PIB-40-C chemiresistors to TCE, trans-DCE, and m-xylene noted in Figure 11 take on additional value. Although only two of the three polymers are different from those used in Figure 10, the analyte discrimination capabilities displayed are significantly different. Rather than having data from all three analytes clumped together in the center with no separation, the data for TCE, trans-DCE, and m-xylene can be seen as three distinct regions. Although the strong and comparable responses from all three chemiresistors place the data from trans-DCE near the middle of the plot, the distinctly different relative magnitudes of response for the other two analytes allow for separation of data. As noted in Figure 11, the strong response of PIB-40-C to TCE places the data points for this analyte in the upper-middle area of the plot, corresponding to higher values on the PIB-40-C axis. The data points for m-xylene show not only the strong response from

PECH-40-C, but also the small magnitude of response from the PCP-40-C, as they are shifted to the right, corresponding to higher values on the PECH-40-C axis and lower values on the PCP-40-C axis. Data points representing exposures of 1% saturated vapor pressure of m-xylene are also lower on the “globe” plot than the rest of the data points for m-xylene, due to the relatively small magnitude response to the low concentrations from the PIB-40-C chemiresistor. Higher concentrations of m-xylene, for which the PIB-40-C response is larger on a relative scale, therefore are shifted to correspond to higher values on the PIB-40-C axis.

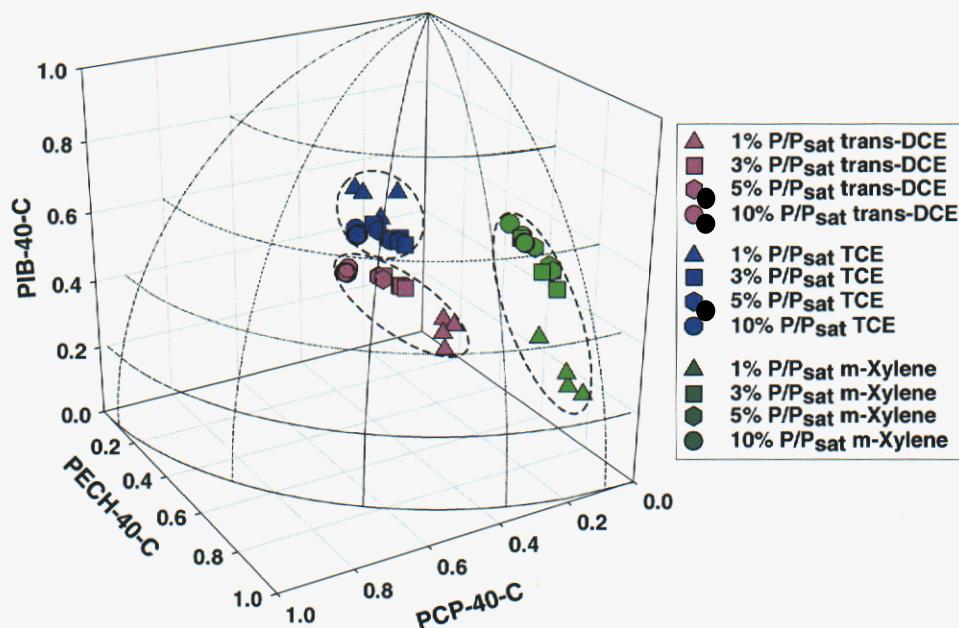


Figure 12. Globe Plot for PCP-40-C, PECH-40-C, and PIB-40-C.

This plot allows for greater separation of the data for trans-DCE, TCE, and m-xylene that were grouped in the middle of Figure 10 (data shown only for these three analytes for clarity). Differences in relative magnitude of response for the three analytes, shown in Figure 11, allow for greater chance of analyte discrimination. The small relative response to m-xylene from PCP-40-C shown in Figure 11 allows for significant separation of the m-xylene data from the other analytes. The stronger response to TCE and trans-DCE from PIB-40-C and PECH-40-C, respectively, is also shown by separation of these two analytes.

Beyond the use of the “globe” plots, an additional tool was used to evaluate the capability of the chemiresistors to identify a given analyte based on the experimental data taken. The visual-empirical region of influence (VERI) technique, a pattern recognition algorithm developed at Sandia, was used to evaluate the quality of the data obtained [18]. Like the “globe” plots, VERI, using some of the same principles of data equalization and normalization, can provide graphical images of data from a number of analytes and sensors; however, unlike the “globe” plots, VERI is not limited to only three sensors at a time. Instead, VERI is capable of allowing a user to see the results of n-dimensional sensor data projected onto a two-dimensional space, and to observe patterns of data clusters through adjustment of the perspective to the data projection. VERI also allows a quantification of data consistency and pattern recognition capabilities through a “leave-one-out” method of analysis, through which each data point in turn is removed from the provided

set of data, and compared to the remainder of the data. The VERI algorithm then rates each data point as being correctly identified as a member of its respective class (i.e., the analyte), an outlier of its respective class, or an unreliable data point that could possibly be incorrectly identified as a member of multiple classes. The evaluation process employed by VERI is based on the same methods used by humans to visually recognize groups or patterns in distributed systems. The quantification capabilities of VERI allow the user to compare pattern recognition capabilities for a given set of sensors and select an optimized array of chemiresistors.

As shown in Table 2, the VERI software was used to quantify the consistency of the equalized and normalized data presented in Figure 10. When only PIB-40-C, PDPP-40-C, and PEVA-40-C are used to detect all six analytes, 62.5% of the data points were correctly identified with their respective class. With 37.5% of the data points considered either outliers or unreliable points that could be identified incorrectly, it is interesting to note that while m-xylene and MTBE have respectively the highest (25%) and lowest (0%) percentages of potentially multiply classed data, as expected based on their placements on the “globe” plot, TCE shows the highest percentage of correctly identified data points. Apparently, although not immediately obvious in Figure 10, while the TCE points are grouped closely with data points for two other analytes, the consistency of placement of the TCE data points allows three-quarters of them to be unambiguously identified.

Table 2. Results of the VERI Analysis for Data Presented in Figure 10.

	Isooctane	Kerosene	MTBE	trans-DCE	TCE	m-Xylene	Total
% Correct	62.50	62.50	68.75	68.75	75.00	37.50	62.50
% Outliers	31.25	25.00	31.25	12.50	12.50	37.50	25.00
% Unreliable	6.25	12.50	0	18.75	12.50	25.00	12.50

The enhanced analyte discrimination for m-xylene, TCE, and trans-DCE shown in Figure 12 can also be seen in the VERI analysis of this data. Table 3, summarizing the VERI analysis of the equalized and normalized responses for PIB-40-C, PCP-40-C, and PECH-40-C to these three analytes, indicates that 75% of the total data points were correctly identified with their respective analyte. Furthermore, none of the data points were considered unreliable, or in danger of being confused with another analyte.

Table 3. Results of the VERI Analysis for Data Presented in Figure 12.

	trans-DCE	TCE	m-Xylene	Total
% Correct	81.25	75.00	68.75	75.00
% Outliers	18.75	25.00	31.25	25.00
% Unreliable	0	0	0	0

By using VERI to examine all possible subsets of chemiresistors, an optimum array can be determined. As shown in Table 4, the best results are obtained from an array of four chemiresistors. Although this may initially seem counterintuitive, the conclusion is consistent

with previously published findings [18], and can be seen as a result of the increase in the percentage of data points unreliably identified through the inclusion of the fifth chemiresistor. The optimized four ink chemiresistor array excludes PIB-40-C. Inclusion of this chemiresistor causes some data points for isooctane and kerosene to be placed in such proximity that they are identified as potentially belonging to both analyte classes.

Table 4. Results of VERI Analysis to Determine the Optimum Chemiresistor Array Size

<u>Chemiresistors in Array</u>	<u>Total % Correct</u>	<u>Total % Outliers</u>	<u>Total % Unreliable</u>
2	71.88	20.83	7.29
3	81.25	16.67	2.08
4	82.29	17.71	0
5	79.17	13.54	7.29

Conclusions

The purpose of this small program was to demonstrate the effectiveness of our vapor phase chemiresistor technology to measuring VOC contamination in water. The chemiresistors were found to measure the higher concentrations of VOC quite easily; the rule of thumb is that the best chemiresistor for a particular VOC can measure down to about 0.1% of the saturated vapor pressure of the liquid VOC at ambient temperature. An example for m-xylene can be seen in Figure 7. Depending on the solubility of the VOC in water, this could be a few ppb in the water. For more soluble VOCs like MTBE, it means a few ppm would be the limit of detection. We were able to detect contamination in water actually touching the chemiresistor polymer, but because of slowness of response and long term instability, it was determined that the chemiresistors work best sensing the headspace vapor of contaminated water. The use of a GORE-TEX® membrane and small dead volume inside the sensor housing means that equilibration between water and the chemiresistors can be fairly rapid. The fastest response was obtained when active sparging forced contaminated headspace vapor past the chemiresistor; this makes sense, as it forces the equilibration (partitioning) between the three phases present, the water, the headspace and the chemiresistor polymer.

References

- [1] Freund, M. S.; Lewis, N. S. *Proc. Natl. Acad. Sci. USA* **1995**, *92*, 2652.
- [2] Lonergan, M. C.; Severin, E. J.; Doleman, B. J.; Beaver, S. A.; Grubbs, R. H.; Lewis, N. S. *Chem. Mater.* **1996**, *8*, 2298.
- [3] Osbourn, G. C.; Bartholemew, J. W.; Ricco, A. J.; Frye, G. C. *Acc. Chem. Res.* **1998**, *31*, 297.
- [4] Nagle, H. T.; Schiffman, S. S.; Gutierrez-Osuna, R. *IEEE Spectrum*, **1998**, *35*, 22.
- [5] Domanský, K.; Baldwin, D. L.; Grate, J. W.; Hall, T. B.; Li, J.; Josowicz, M.; Janata, J. *Anal. Chem.* **1998**, *70*, 473.
- [6] Zellers, E. T.; Han, M. *Anal. Chem.* **1996**, *68*, 2409.
- [7] Eastman, M. P.; Hughes, R. C.; Yelton, W. G.; Ricco, A. J.; Patel, S. V.; Jenkins, M. W. "Application of the Solubility Parameter Concept to the Design of Chemiresistor Arrays," *J. Electrochem. Soc.* **1999**, *146*, 3907.
- [8] Hughes, R. C.; Eastman, M. P.; Yelton, W. G.; Ricco, A. J.; Patel, S. V.; Jenkins, M. W. *Tech. Digest of the 1998 Solid-State Sensor and Actuator Workshop*, Transducers Research Foundation: Cleveland, 1998, pp. 379-382.
- [9] Hampl, J.; Bouda, V. *Synthetic Metals*, **1994**, *67*, 129.
- [10] Heaney, M. B. *Appl. Phys. Lett.* **1996**, *69*, 2602.
- [11] Heaney, M. B. *Physica A*, **1997**, *241*, 296.
- [12] Ballantine, D. S.; Rose, S. L.; Grate, J. W.; Wohltjen, H. *Anal. Chem.* **1986**, *58*, 3058.
- [13] McGill, R. A.; Abraham, M. H.; Grate, J. W. *Chemtech* **1994**, *24*, 27.
- [14] Viswanathan, R.; Heaney, M. B. *Phys. Rev. Lett.* **1995**, *75*, 4433.
- [15] Grate, J. W.; Kaganove, S. N.; Bhethanabotla, V. R. *Anal. Chem.* **1998**, *70*, 199.
- [16] Mackay, D.; Shiu, W. Y. *J. Phys. Chem. Ref. Data*, **1981**, *10*, 1175.
- [17] Patel, S. V.; Jenkins, M. W.; Hughes, R. C.; Yelton, W. G.; Ricco, A. J. *Anal. Chem.* **2000**, *72*, 1532.
- [18] Osbourn, G. C.; Bartholomew, J. W.; Bouchard, A. M.; Martinez, R. F. www.sandia.gov/imrl/XVisionScience/Xusers.htm.

APPENDIX - Responses to Questions from SERDP Reviewers

Material used to develop this report was presented to a panel of reviewers from the Strategic Environmental Research and Development Program (SERDP). This presentation took place as part of the work performed through funding provided through the SERDP Exploratory Development (SEED) effort. The reviewers had several questions or requests for additional information about the use of chemiresistors for detection of ground water contamination. This appendix contains their questions/comments and the respective answers.

1. Describe how the sensor would be deployed in the field. Include a discussion of the type of wells that can be used, well purging, and placement of sensors.

Fortunately for this program, we were able to obtain internal funding at Sandia in FY01 to push the development of this sensor technology for soil monitoring. The probe we designed for these experiments has a GORE-TEX® membrane and a waterproof cable, so it turns out it can work in soil, high humidity and even in liquid water. Many details about this probe can be found on our web page, www.sandia.gov/sensor. There have been a number of recent field trials, including field deployment of the chemiresistor sensor probe at the Sandia Chemical Waste Landfill some 60 feet down an existing well, and using an existing surface data logger (only electrical resistances need to be measured, so no electronics is required downhole, a big advantage to this technology). There was also a proof test in a 55-gallon drum at the HAZMAT Spill Center at the Nevada Test Site to test the sensor during a trichloroethylene spill and air-venting remediation operation. Other tests are planned, but funding for them must be obtained.

2. Discuss any additional development work being conducted on the sensors that is funded by different agencies.

A press release from Sandia in Sept. 2001 on our Laboratory Directed Research and Development (LDRD)-funded probe for soil and groundwater monitoring has received a tremendous amount of attention from the media, partly because it coincided with the events of September 11th, leading to worries about the safety of water supplies. As a result, we have signed non-disclosure agreements with several companies who might commercialize this technology (names can not be revealed at this time due to on-going negotiations). A significant amount of funding will be needed to turn this laboratory prototype sensor into a commercial product. We have three patent applications filed for intellectual property protection of several aspects of the technology. However, the standardization of the chemiresistor inks and reproducible manufacturing will require some effort, which the future licensees should undertake. We were able to secure LDRD funding for FY02 to continue research and development on the technology even though the SEED program has now (01/02) been finished. There are many unanswered questions about the performance of the sensors in realistic environments. Even 60 feet down a well there are significant temperature variations over a period of days. The actual local relative humidity in soil at these depths has not been determined, or how the

chemiresistor sensor will respond to it. We hope that a combination of funding sources, including SERDP and the potential licensees, among others, can be put together to push this very promising technology forward to application in the field.